Supporting Information

Hybrid Transition Metal Nanocrystals-Embedded Graphitic Carbon Nitride Nanosheets System as Superior Oxygen Electrocatalyst for Rechargeable Zn-Air Batteries

Wen-Jun Niu, Jin-Zhong He, Ya-Ping Wang, Qiao-Qiao Sun, Wen-Wu Liu, Lu-Yin Zhang, Mao-Cheng Liu, Ming-Jin Liu, Yu-Lun Chueh**

Prof. W. J. Niu, J. Z. He, Y.P. Wang, Q.-Q. Sun, Prof. W. W Liu, L. Y. Zhang, and M. C. Liu, State Key Laboratory of Advanced Processing and Recycling of Non-ferrous Metals, Lanzhou University of Technology, Lanzhou 730050, P. R. China.

School of Materials Science and Engineering, Lanzhou University of Technology, Lanzhou 730050, P. R. China.

**Email: niuwenjun@lut.edu.cn*

M. J. Liu, Prof. Y.-L. Chueh

Department of Materials Science and Engineering, National Tsing Hua University, Hsinchu, 30013, Taiwan.

Department of Physics, National Sun Yat-Sen University, Kaohsiung, 80424, Taiwan.

Frontier Research Center on Fundamental and Applied Sciences of Matters, National Tsing Hua University, Hsinchu 30013, Taiwan.

**Email: ylchueh@mx.nthu.edu.tw*

Table S1 A summary of various electrocatalysts for ORR and OER performance.

Electrocatalysts	ORR		OER	ΔE (V)	Ref.
	$E_{1/2}$ (V)	E_0 (V)	$E_{j=10}$ (V)		
Co-N-C$_{-0.7}$	**0.803**	**0.875**	**1.67**	**0.867**	**This work**
Fe-N-C$_{-0.7}$	**0.781**	**0.887**	**1.71**	**0.929**	**This work**
Ni-N-C$_{-0.7}$	**0.765**	**0.889**	**1.62**	**0.855**	**This work**
Co/$CoFe_2O_4$	0.63	0.77	1.62	0.99	[1]
Mn/Co-N-C-0.02- 800	0.80	—	1.66	0.86	[2]
Ni_3Fe-Co_9S_8/rGO	0.80	—	1.62	0.82	[3]
NDGs-800	0.85	0.98	1.68	0.83	[4]
Co_2P/CoN-in-NCNTs	0.85	—	1.65	0.80	[5]
N-HC@G-900	0.65	0.80	1.58	0.93	[6]
C@NCF-900	0.93	—	1.66	0.73	[7]
NiCo/MNC	0.83	—	1.61	0.78	[8]
Fe_2Ni_2N/Co@NCNT	0.76	—	1.63	0.87	[9]
NB-CN	0.835	—	1.65	0.815	[10]
CoZn-NC-700	0.84	0.98	1.76	0.78	[11]
HNG-900	0.78	—	1.69	0.91	[12]
N-GCNT/FeCo-3	0.92	—	1.73	0.81	[13]
CoNC-CNF-1000	0.8	—	1.68	0.88	[14]
Co/N-HPC150/800	0.85	—	1.7	0.85	[15]
CoFe-PPy	0.84	—	1.69	0.85	[16]
CN_x	0.68	—	1.62	0.94	[17]

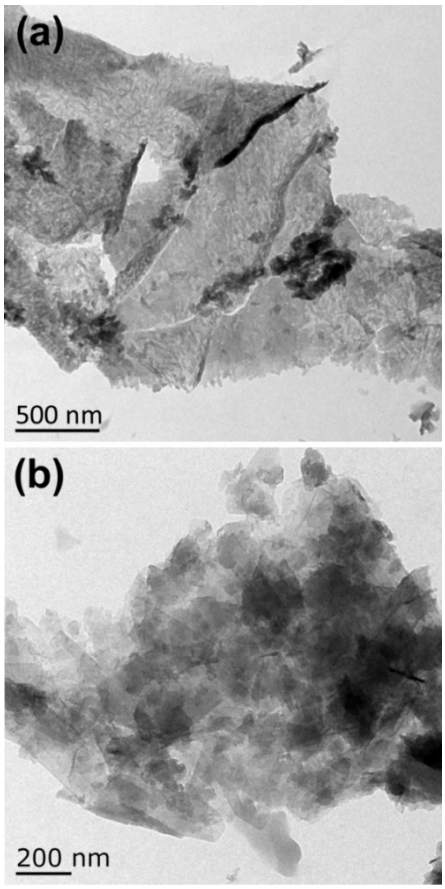

Figure S1 TEM images of the (a) bulk *g*-C_3N_4 and (b) *g*-C_3N_4 nanosheets.

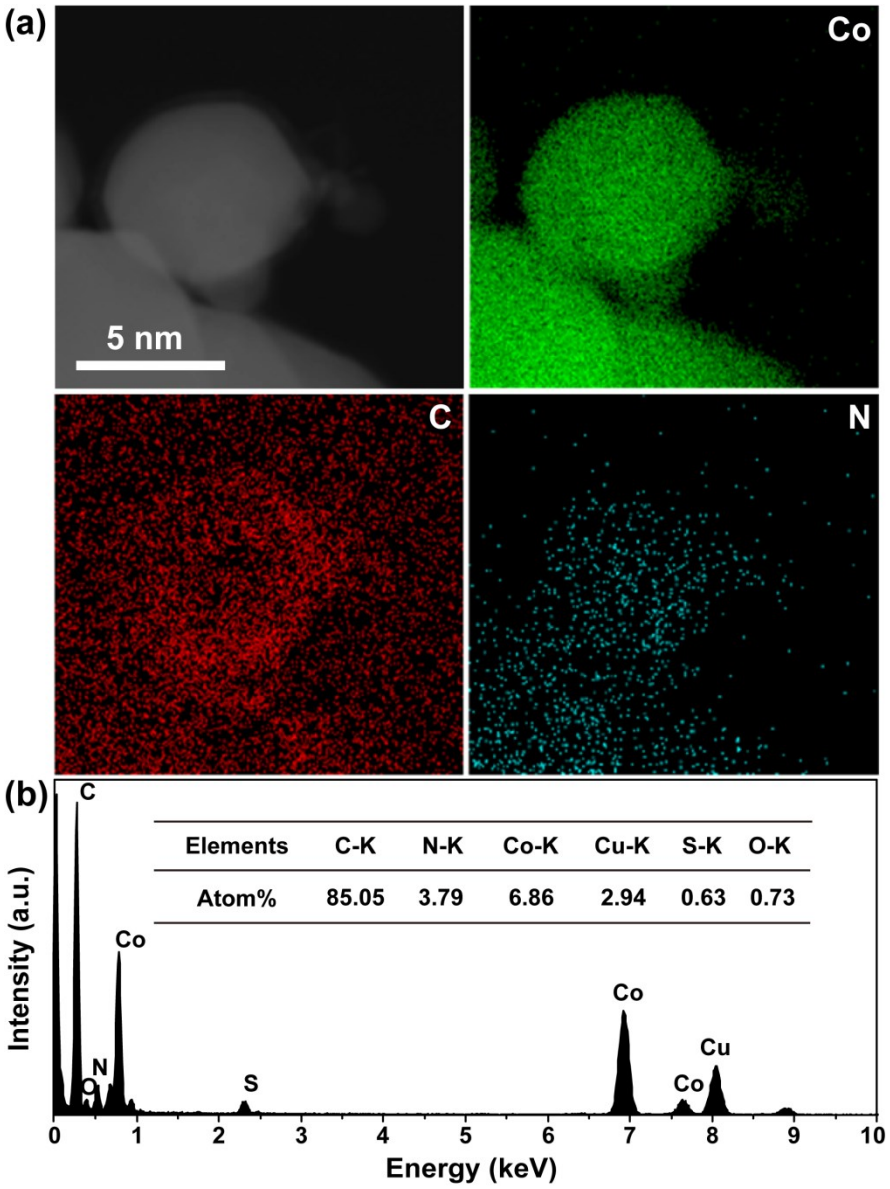

Figure S2 (a) The EDS element mapping of C, Co, N, and (b) the corresponding spectrum of the Co-CNNs$_{-0.7}$ composites.

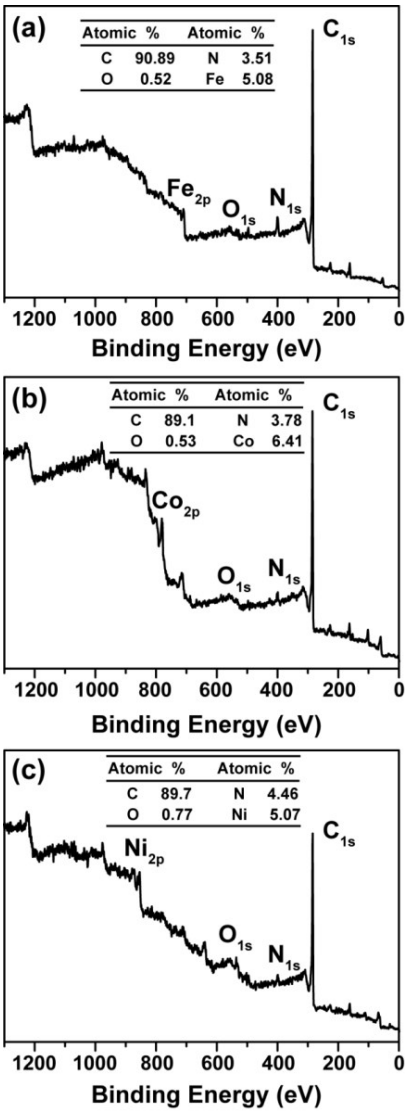

Figure S3 XPS survey spectra of the (a) Fe-CNNs$_{-0.7}$, (b) Co-CNNs$_{-0.7}$, and (c) Ni-CNNs$_{-0.7}$, respectively.

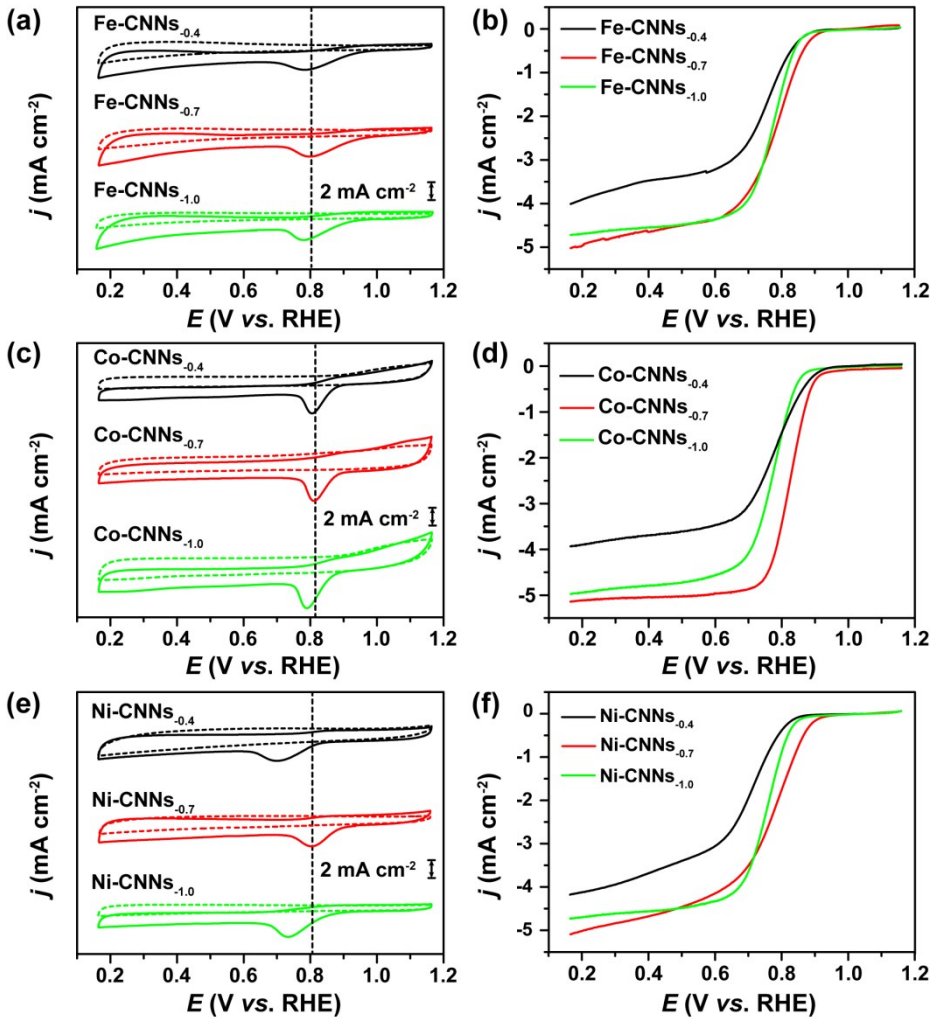

Figure S4 CVs and LSV curves of (a, b) Fe-CNNs with different Fe ions doping, (c, d) Co-CNNs with different Co ions doping, and (c, f) Ni-CNNs with different Ni ions doping in O_2-saturated 0.1 M KOH (1600 rpm, 5 mV s^{-1}).

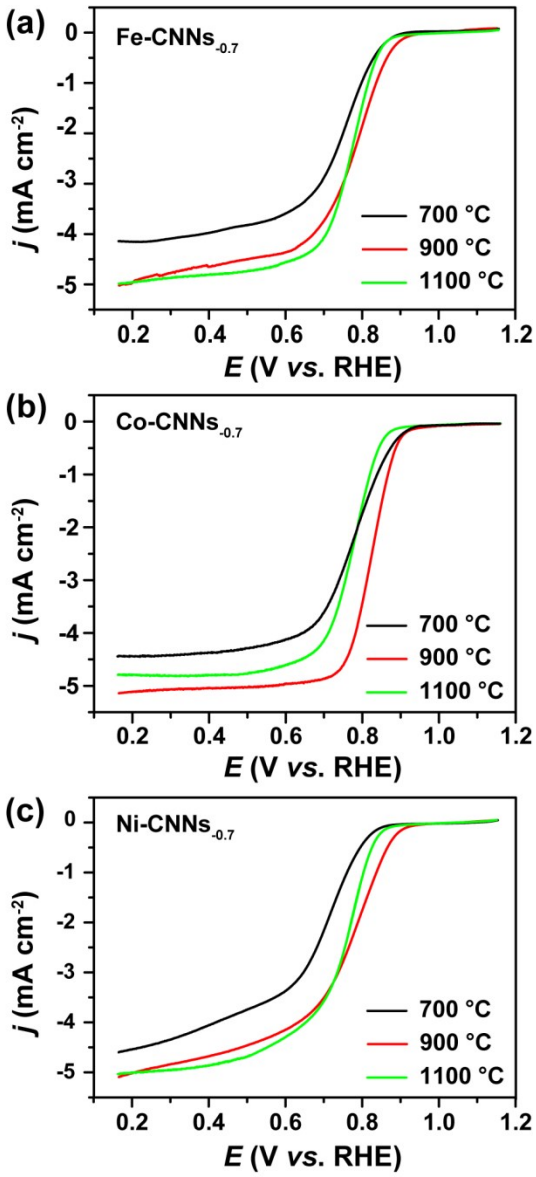

Figure S5 ORR polarization plots of (a) Fe-CNNs$_{-0.7}$, (b) Co-CNNs$_{-0.7}$, and (c) Ni-CNNs$_{-0.7}$ catalysts pyrolyzed at different temperatures in O_2-saturated 0.1 M KOH (1600 rpm, 5 mV s^{-1}).

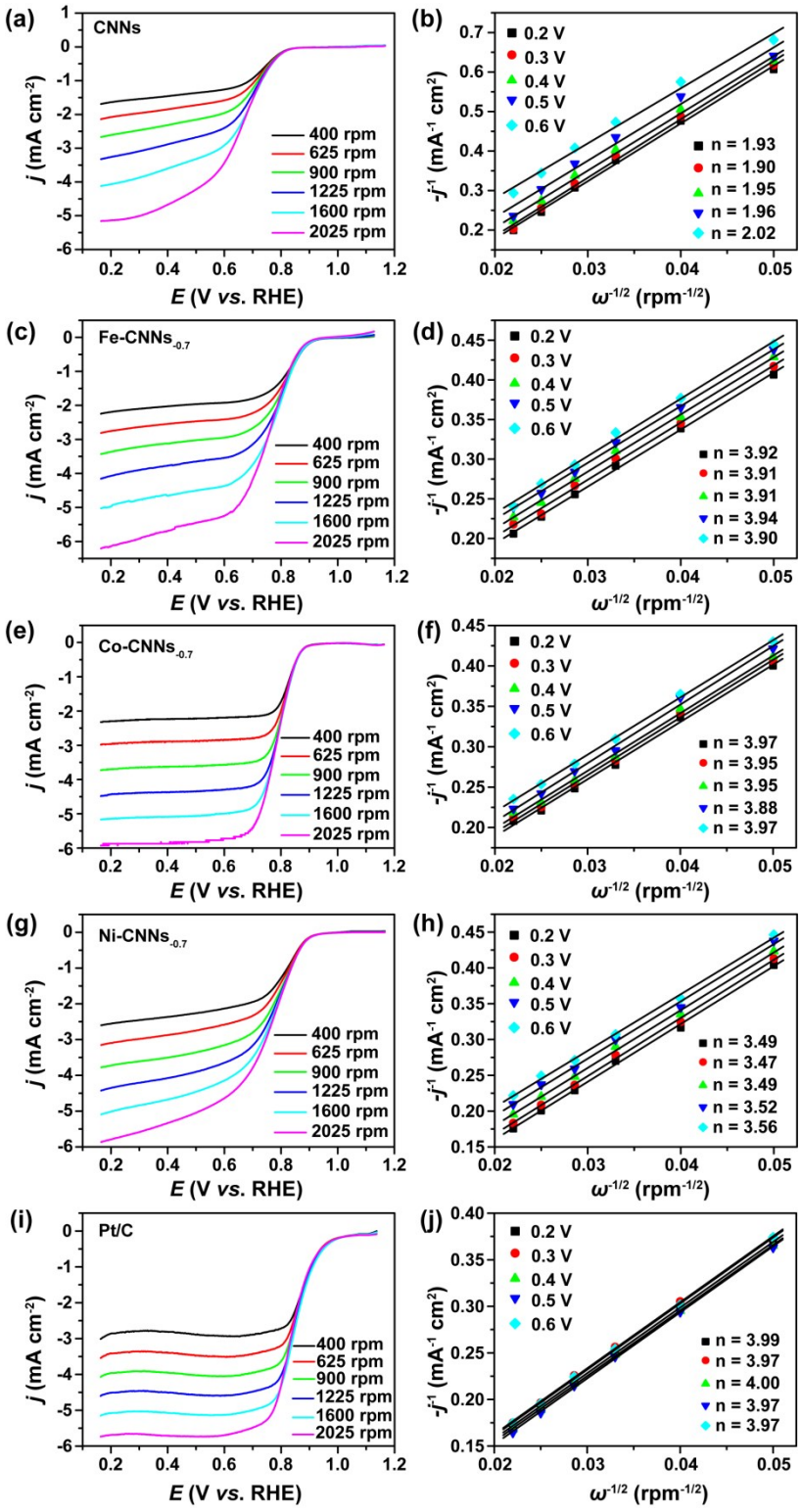

Figure S6 LSV curves and Koutecky–Levich plots (j^{-1} versus $\omega^{-1/2}$) of (a, b) CNNs, (c, d) Fe-CNNs$_{-0.7}$, (e, f) Co-CNNs$_{-0.7}$, (g, h) Ni-CNNs$_{-0.7}$ and (i, g) Pt/C electrodes in O_2-saturated 0.1 M KOH solution at a series of rotation rates from 400 to 2025 rpm with a scan rate of 5 mV s^{-1}.

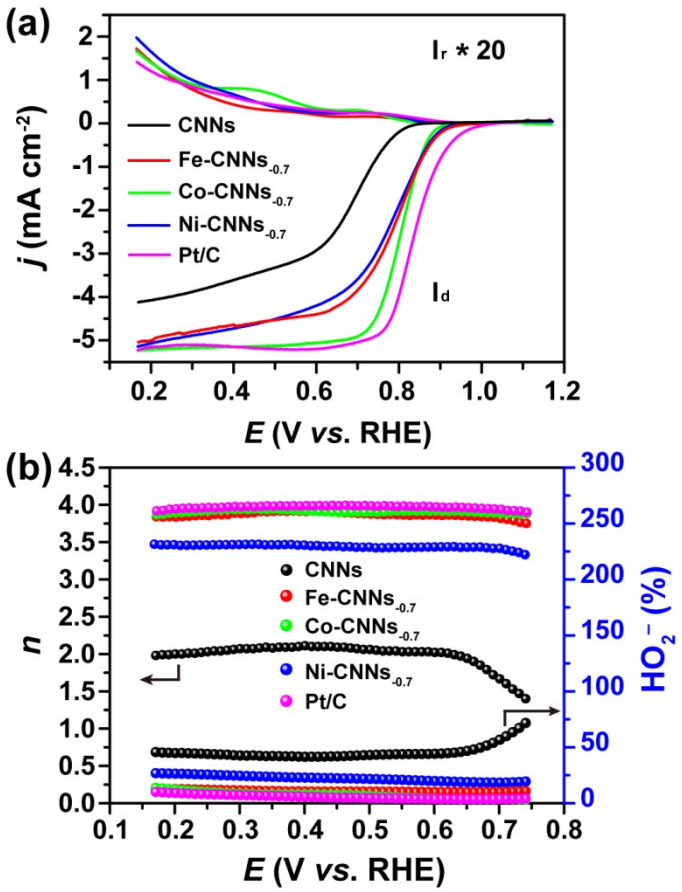

Figure S7 (a) RRDE voltammograms recorded and (b) Peroxide species yields and electron numbers of CNNs, Fe-CNNs$_{-0.7}$, Co-CNNs$_{-0.7}$, Ni-CNNs$_{-0.7}$, and Pt/C electrodes in O_2-saturated 0.1 M KOH at 1600 rpm.

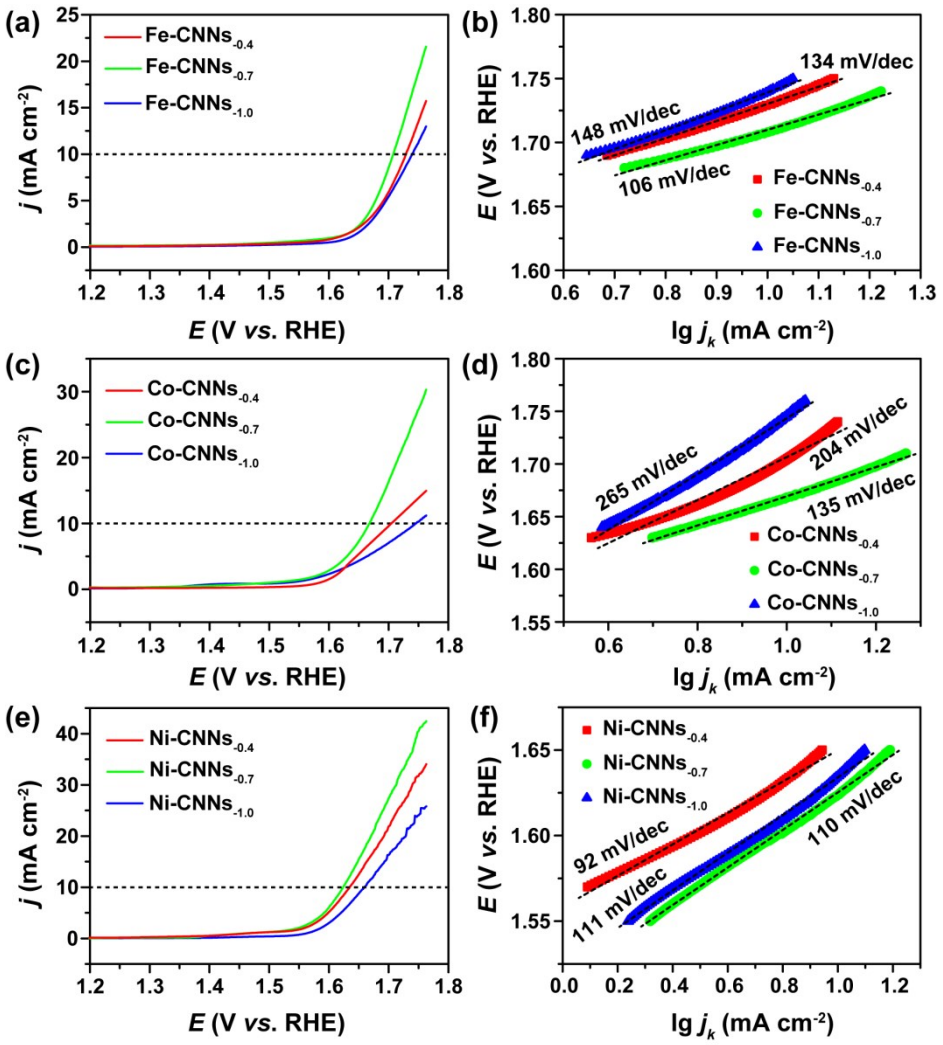

Figure S8 LSV and Tafel plots of (a, b) Fe-CNNs with different Fe ions doping, (c, d) Co-CNNs with different Co ions doping, and (c, f) Ni-CNNs with different Ni ions doping in O_2-saturated 0.1 M KOH (1600 rpm, 5 mV s^{-1}).

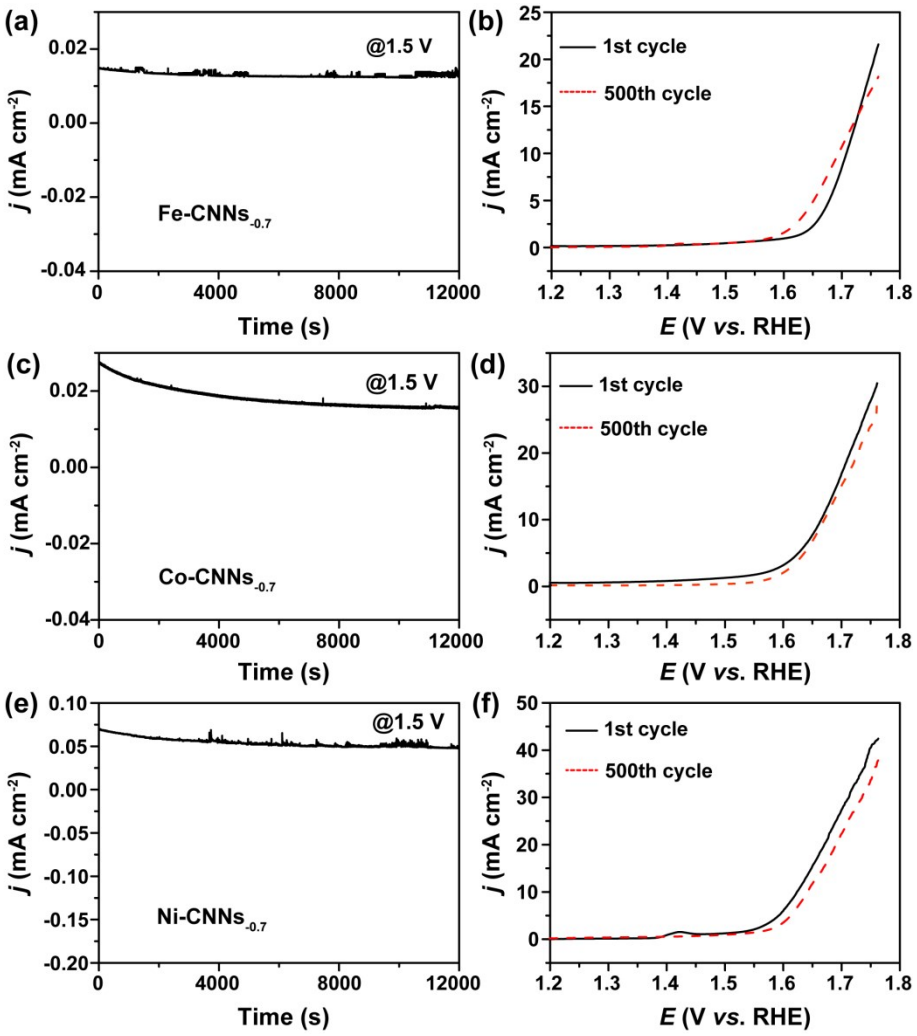

Figure S9 Chronoamperometry responses and the LSV curves before and after 500 CV cycles of the (a, b) Fe-CNNs$_{-0.7}$, (c, d) Co-CNNs$_{-0.7}$, as well as (e, f) Ni-CNNs$_{-0.7}$ in O_2-saturated 0.1 M KOH electrolyte (1600 rpm, 5 mV s^{-1})

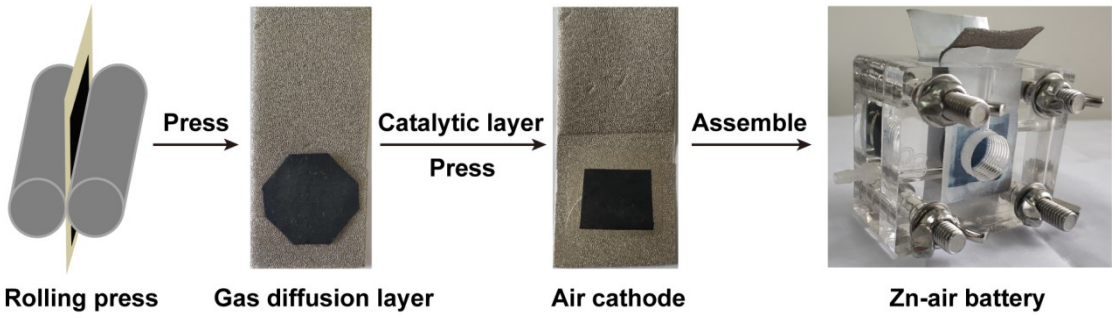

Figure S10 Schematic illustration for the preparation of gas diffusion layer, air-cathode loaded with catalysts and the assembly of rechargeable Zn-air battery.

The home-made Zn-air batteries were constructed using a polished Zn plate as the anode, the air electrode composed of nickel foam (0.1 mm), catalytic layer (CL) and gas diffusion layer (GDL) as cathode, and 6 M KOH aqueous solution containing 0.2 M $Zn(Ac)_2$ as electrolyte. Typically, the CL was fabricated by mixing catalysts ($Co\text{-}CNNs_{-0.7}$), conductive additive (ketjen black and acetylene black) and binder (PTFE, 60 wt.%) uniformly in a weight ratio of 3 : 3 : 1 : 3. While the GDL was fabricated by rolling press the acetylene black, ammonium oxalate and PTFE hybrid slurry in a weight ratio of 2 : 1 : 7. Finally, the total thickness of the air electrode was 0.4 to 0.6 mm after pressed at 10 MPa. Then, the air electrode was dried at 60 °C in a vacuum overnight.

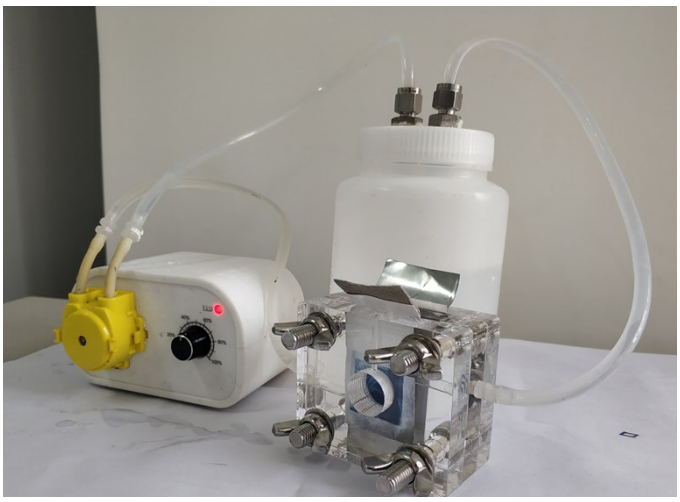

Figure S11 Photograph of the rechargeable Zn-air battery.

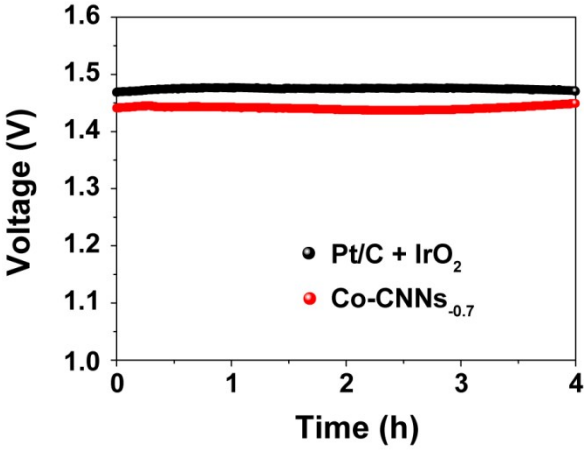

Figure S12 Open circuit plots of the rechargeable ZABs with the Co-CNNs$_{-0.7}$ and Pt/C + IrO_2 as catalyst, respectively.

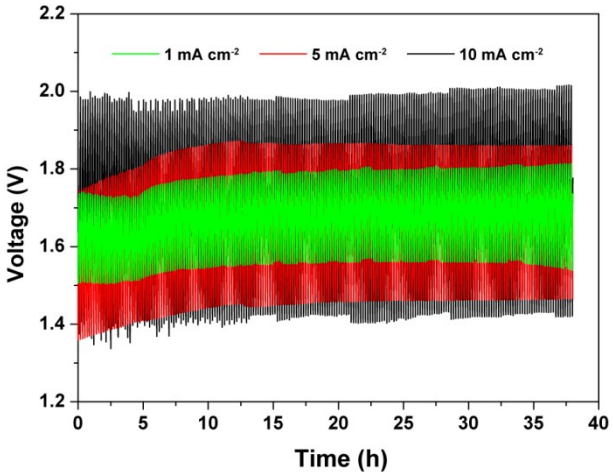

Figure S13 Galvanostatic discharge/charge cycling curves of the ZABs equipped with the Co-CNNs$_{-0.7}$ at 1 mA cm^{-2}, 5 mA cm^{-2} and 10 mA cm^{-2}, respectively.

References

[1] Y. Niu, X. Huang, L. Zhao, W. Hu and C. M. Li, One-Pot Synthesis of Co/$CoFe_2O4$ Nanoparticles Supported on N-Doped Graphene for Efficient Bifunctional Oxygen Electrocatalysis, *ACS Sustainable Chem. Eng.* **2018**, 6, 3556.

[2] L. Wei, L. Qiu, Y. Liu, J. Zhang, D. Yuan and L. Wang, Mn-Doped Co-N-C Dodecahedron as a Bifunctional Electrocatalyst for Highly Efficient Zn–Air Batteries, *ACS Sustainable Chem. Eng.* **2019**, 7, 16, 14180.

[3] X. Hu, T. Huang, Y. Tang, G. Fu and J. M. Lee, Three-Dimensional Graphene-Supported Ni_3Fe/Co_9S_8 Composites: Rational Design and Active for Oxygen Reversible Electrocatalysis, *ACS Appl. Mater. Interfaces* **2019**, 11, 4028.

[4] Q. Wang, Y. Ji, Y. Lei, Y. Wang, Y. Wang, Y. Li and S. Wang, Pyridinic-N-Dominated Doped Defective Graphene as a Superior Oxygen Electrocatalyst for Ultrahigh-Energy-Density Zn-Air Batteries, *ACS Energy Lett.* **2018**, 3, 5, 1183.

[5] Y. Guo, P. Yuan, J. Zhang, H. Xia, F. Cheng, M. Zhou, J. Li, Y. Qiao, S. Mu and Q. Xu, Co_2P-CoN double active centers confined in N-doped carbon nanotube: heterostructural engineering for tri-functional catalysis toward HER, ORR, OER, and Zn-air batteries driven water splitting, *Adv. Funct. Mater.* **2018**, 28, 1805641.

[6] J. Sun, S. E. Lowe, L. Zhang, Y. Wang, K. Pang, Y. Wang, Y. Zhong, P. Liu, K. Zhao, Z. Tang and H. Zhao, Ultrathin Nitrogen-Doped Holey Carbon@Graphene Bifunctional Electrocatalyst for Oxygen Reduction and Evolution Reactions in Alkaline and Acidic Media, *Angew. Chem. Int. Ed.* **2018**, 57, 16511.

[7] G. Nam, Y. Son, S. O. Park, W. C. Jeon, H. Jang, J. Park, S. Chae, Y. Yoo, J. Ryu, M. G.

Kim, S. K. Kwak and J. Cho, A Ternary $Ni_{46}Co_{40}Fe_{14}$ Nanoalloy-Based Oxygen Electrocatalyst for Highly Efficient Rechargeable Zinc-Air Batteries, *Adv. Mater.* **2018**, 30, 1803372.

[8] D. Deng, Y. Tian, H. Li, L. Xu, J. Qian, J. Pang, B. Wang, Q. Zhang and H. Li, *J Alloy Compd.* **2019**, 797, 1041.

[9] M. Wu, G. Zhang, J. Qiao, N. Chen, W. Chen, S. Sun, Ultra-long life rechargeable zinc-air battery based on high-performance trimetallic nitride and NCNT hybrid bifunctional electrocatalysts, *Nano Energy* **2019**, 61, 86.

[10] Z. Lu, J. Wang, S. Huang, Y. Hou, Y. Li, Y. Zhao, S. Mu, J. Zhang, Y. Zhao, N,B-codoped defect-rich graphitic carbon nanocages as high performance multifunctional electrocatalysts, *Nano Energy* **2017**, 42, 334.

[11] B. Chen, X. He, F. Yin, H. Wang, D. J. L, R. Shi, J. Chen and H. Yin, MO-Co@N-Doped Carbon (M = Zn or Co): Vital Roles of Inactive Zn and Highly Efficient Activity toward Oxygen Reduction/Evolution Reactions for Rechargeable Zn-Air Battery, *Adv. Funct. Mater.* **2017**, 27, 1700795.

[12] H. Cui, M. Jiao, Y. N. Chen, Y. Guo, L. Yang, Z. Xie, Z. Zhou and S. Guo, Molten-Salt-Assisted Synthesis of 3D Holey N-Doped Graphene as Bifunctional Electrocatalysts for Rechargeable Zn-Air Batteries, *Small Methods* **2018**, 2, 1800144.

[13] C. Y. Su, H. Cheng, W. Li, Z. Q. Liu, N. Li, Z. Hou, F. Q. Bai, H. X. Zhang and T. Y. Ma, Atomic Modulation of FeCo-Nitrogen-Carbon Bifunctional Oxygen Electrodes for Rechargeable and Flexible All-Solid-State Zinc-Air Battery, *Adv. Energy Mater.* **2017**, 7, 1602420.

[14] W. Zhang, X. Yao, S. Zhou, X. Li, L. Li, Z. Yu and L. Gu, ZIF-8/ZIF-67-Derived Co-N_x-Embedded 1D Porous Carbon Nanofibers with Graphitic Carbon-Encased Co Nanoparticles as an Efficient Bifunctional Electrocatalyst, *Small* **2018**, 14, 1800423.

[15] F. Dong, C. Liu, M. Wu, J. Guo, K. Li and J. Qiao, Hierarchical Porous Carbon Derived from Coal Tar Pitch Containing Discrete Co-Nx-C Active Sites for Efficient Oxygen Electrocatalysis and Rechargeable Zn-Air Batteries, *ACS Sustainable Chem. Eng.* **2019**, 7, 8587.

[16] P. Li, Z. Jin, Y. Qian, Z. Fang, D. Xiao and G. Yu, Probing Enhanced Site Activity of Co-Fe Bimetallic Subnanoclusters Derived from Dual Cross-Linked Hydrogels for Oxygen Electrocatalysis, *ACS Energy Lett.* **2019**, 4, 1793.

[17] K. Mamtani, D. Jain, D. Dogu, V. Gustin, S. Gunduz, A. C. Co and U. S. Ozkan, Insights into oxygen reduction reaction (ORR) and oxygen evolution reaction (OER) active sites for nitrogen-doped carbon nanostructures (CN_x) in acidic media, *Appl. Catal. B-Environ.* **2018**, 220, 88.